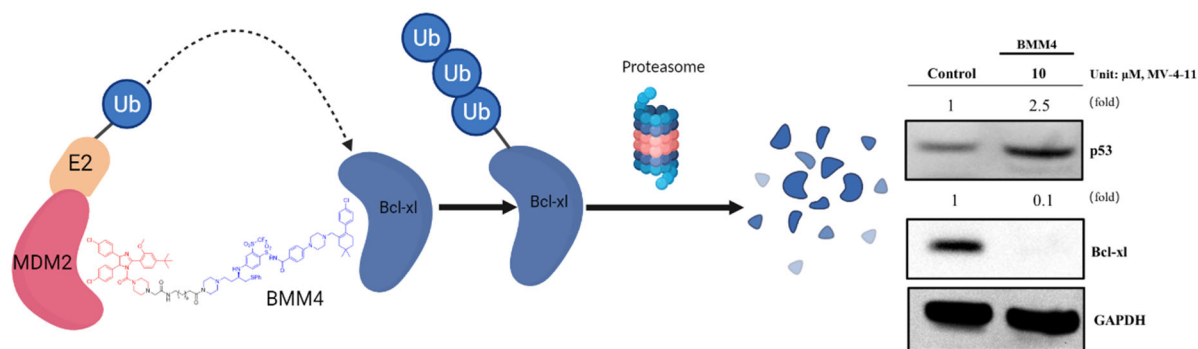


MDM2-BCL-X_L PROTACs enable degradation of BCL-X_L and stabilization of p53

Authors: Mengyang Chang, Feng Gao, Jing Chen, Giri Gnawali, and Wei Wang

Graphical abstract



Highlights

1. The first MDM2-Bcl-X_L PROTACs were developed.
2. Compound **BMM4** was identified showing potent degradation activity toward Bcl-X_L and stabilization of p53.
3. The combination of **BMM4** with ABT-199 exhibited a synergic anticancer activity.

In brief

BMM4 is the first MDM2-Bcl-X_L PROTAC, which showed unique antiproliferative activity and could serve as a potential anti-cancer agent for the further development.

MDM2-BCL-X_L PROTACs enable degradation of BCL-X_L and stabilization of p53

Mengyang Chang^a, Feng Gao^b, Jing Chen^b, Giri Gnawali^b, and Wei Wang^{a,b,*}

^a Department of Chemistry and Biochemistry, University of Arizona, Tucson, AZ, USA.

^b Department of Pharmacology and Toxicology, University of Arizona, Tucson, Az, USA.

*Correspondence: wwang@pharmacy.arizona.edu (W. Wang)

Abstract

Inhibition or degradation of anti-apoptotic protein BCL-X_L is a viable strategy for cancer treatment. Despite the recent development of PROTACs for degradation of BCL-X_L, the E3 ligases are confined to the commonly used VHL and CRBN. Herein we report the development of MDM2-BCL-X_L PROTACs using MDM2 as E3 ligase for degradation of BCL-X_L. Three MDM2-BCL-X_L PROTACs derived from MDM2 inhibitor Nutlin-3, which can also upregulate p53, and BCL-2/BCL-X_L inhibitor ABT-263 with different linker length were designed, synthesized, and evaluated in vitro. We found **BMM4** exhibited potent, selective degradation activity against BCL-X_L and stabilized tumor suppressor p53 in U87, A549 and MV-4-11 cancer cell lines. Moreover, combination of BMM4 and BCL-2 inhibitor ABT-199 showed synergistic antiproliferative activity. The unique dual-functional PROTACs offers an alternative strategy for targeted protein degradation.

Keywords: BCL-X_L, MDM2 E3 ligase, PROTAC, targeted protein degradation

1. Introduction

A hallmark of cancer is the evasion of cellular apoptosis, largely mediated by pro- and antiapoptotic proteins.¹ BCL-X_L and BCL-2 are main participants of the anti-apoptotic BCL-2 protein family.²⁻⁵ The upregulation of the antiapoptotic BCL-2 family proteins induces apoptosis evasion leading to tumor initiation, progression, and resistance to chemo- and targeted therapies.²⁻⁵ BCL-X_L and BCL-2 are well validated cancer targets.⁶⁻⁷ Small-molecule inhibitors of these proteins promote Bax/Bak oligomerization, which leads to permeabilization of the mitochondrial outer membrane, cytochrome c release, and caspase activation, and ultimately leading to apoptosis.²

Navitoclax (ABT-263) is an orally bioavailable small molecule drug that inhibits BCL-2/BCL-X_L selectively and potently, resulting in single-agent efficacy in a preclinical small cell lung cancers (SCLC) model (Figure 1).⁸ ABT-263 inhibition of BCL- X_L causing on-target and dose-limiting thrombocytopenia prevents it from its clinical usage.⁹⁻¹⁰ To address this issue, ABT-263 derived PROTACs using CRBN and VHL ligands as E3 recruitment components have been developed by Zhou and Zheng and showed reduced platelet toxic effects, and potent BCL-X_L selective anti-cancer activity.¹¹⁻¹² The studies imply that the E3 ligands play key roles in degradation activity and selectivity.¹³⁻¹⁵ Different E3 ligases may define a different band region of surface lysine to regulate PROTAC-induced target ubiquitination and degradation.¹⁶ Some E3 ligases have a narrower range of activity and a narrower lysine and substrate selectivity, while others have a broader range of activity and a less defined lysine and substrate selectivity.^{15, 17} Therefore, the development of new BCL-2/ X_L degraders using different E3 ligases may have unique degradation capacity.¹⁸

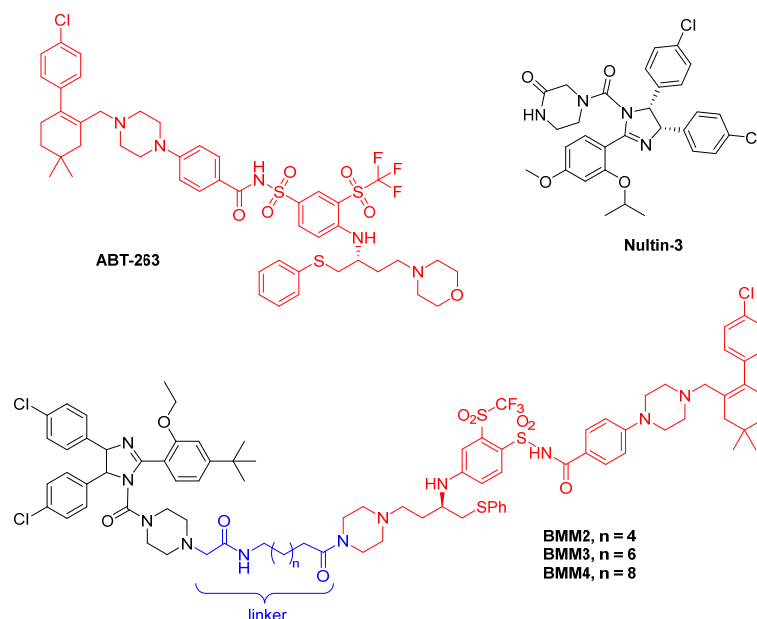


Figure 1. Structures of Bcl-XL/Bcl-2 inhibitor ABT-263, MDM2 inhibitor Nutlin-3, and new MDM2-recruiting, Bcl-xl-degrading PROTACs BMM.

Mouse double minute 2 homolog (MDM2) is an E3 ubiquitin ligase that binds to tumor suppressor p53, causing the subsequent degradation by ubiquitin.¹⁹⁻²⁰ Compared to the other E3 ligases (von Hippel–Lindau (VHL), or cereblon (CRBN)) used in PROTACs, MDM2 is unique in that its endogenous substrate, the tumor suppressor p53, plays a major role in tumor suppression.²¹ In response to the cellular stress, DNA damage, and hypoxia, p53 is upregulated and induces pathways that cause cell cycle arrest, DNA repair, cellular senescence, differentiation, and apoptosis.²²⁻²³ Overexpression of MDM2 can reduce the expression of p53 through the negative feedback pathway.²⁴⁻²⁶ Inhibition of MDM2 protein blocks MDM2-p53 interaction, up-regulates the expression of p53 and thus exerts antitumor activity.²⁷⁻²⁹ Several small-molecule MDM2-p53 inhibitors have entered clinical trials.³⁰⁻³¹

Considering the important roles of BCL-2 and BCL-XL and MDM2 played in cancer, we design PROTACs by incorporation of MDM2 inhibitor into a BCL-2/XL inhibitor (e.g., ABT-263) via a linker. Such unique PROTACs may be capable of degrading BCL-XL and/or BCL-2 and meanwhile inhibiting MDM2 and stabilizing the p53 expression. Herein we wish to report the

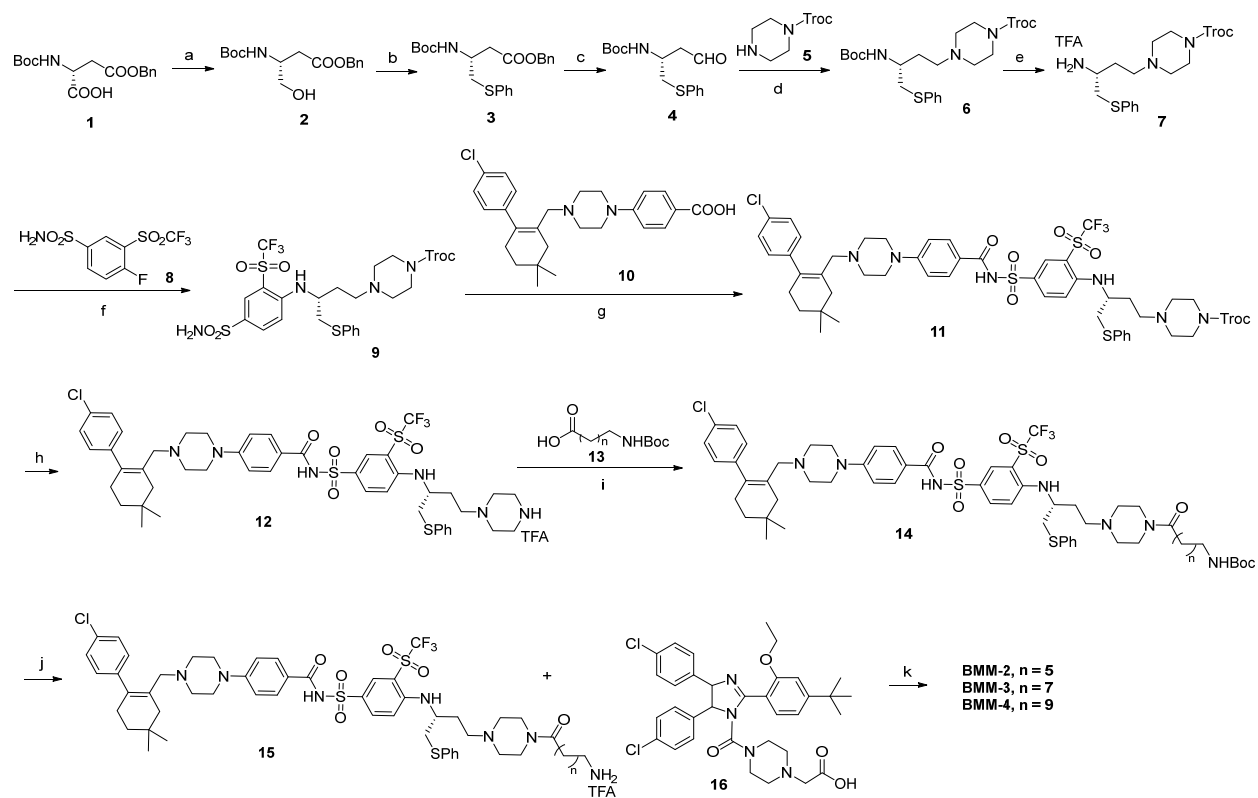
studies that lead to discover dual functional PROTACs, which can selectively degrade BCL-X_L and stabilize p53.

Results

Chemistry

Nutlin-3 (Fig 1b) is a potent MDM2 inhibitor.³² We have developed a homo-PROTAC by connecting two Nutlin-3 ligands through appropriate linkers for the degradation of MDM2.³³ ABT-263 as a ligand was used in the design of CRBN/VHL-based BCL-X_L specific degraders.¹¹⁻¹² Based on the structure information, we designed Nutlin-3 and ABT-263 derived PROTACs BMMs via a linear linker connecting two solvent exposure sites in the two structures (Figure 1). The degradation activity is affected by the structure particularly length of the linker. Therefore, different sized linkers will be synthesized and examined for bioactivity studies.

The route for the synthesis of designed PROTACs is illustrated in Scheme 1. ABT-263 derivative **12** was prepared by following literature procedures.³⁴ Briefly, commercially available aspartic acid derivative **1** was reduced by NaBH₄ to give alcohol **2**, which was then converted to a thioether **3**. The reduction of ester **3** to aldehyde **4** by DIBAL-H at -78 °C was followed by reductive amination with Troc-protected piperazine (**5**) to afford compound **6**. Deprotection of Boc compound **6** led to compound **7**, which underwent aromatic nucleophilic substitution with 4-fluoro-3-((trifluoromethyl)sulfonyl)benzene sulfonamide **8** to give aniline **9**. The key intermediate **12** was achieved *via* amide condensation with compound **10** followed by deprotection. Coupling of piperazine **12** with various length linkers ranging from 6 to 10 carbons and deprotection of Boc yielded amide **15**. Finally, the amidation of the amine **15** with MDM2 inhibitor **16** delivered the target structures **BMM-2-4**.



Scheme 1. Synthesis of **BMM-2-4**. Reagents and conditions: (a) (1) *N*-methylmorpholine, isobutyl chloroformate, THF, $-25\text{ }^{\circ}\text{C}$ then $-15\text{ }^{\circ}\text{C}$; (2) NaBH_4 , H_2O , $-15\text{ }^{\circ}\text{C}$; (b) Bu_3P , diphenyl disulfide, toluene, $80\text{ }^{\circ}\text{C}$; (c) DIBAL-H, toluene, $-78\text{ }^{\circ}\text{C}$; (d) $\text{NaBH}(\text{OAc})_3$, TEA, DCM; (e) TFA, DCM; (f) TEA, acetonitrile, reflux; (g) EDCI, DMAP, DCM; (h) Zn, HOAc, THF; (i) HATU, TEA, DCM; (j) TFA, DCM; (k) HATU, TEA, DMF.

Biological evaluation

BMM-2-4 PROTACs degradation activity in U87 glioblastoma cell lines

The BMM PROTACs are designed for the degradation of Bcl-X_L/Bcl-2. Their degradation ability in cancer cells was evaluated by immunoblotting. The glioblastoma cell line, U87, was selected for initial evaluation of BMM PROTACs given the roles of Bcl-X_L/Bcl-2 in brain cancer.³⁵ U87-MG cells were treated with 1.0 and 10.0 μM of BMM for 24 h. Very limited degradation activity was observed at 1.0 μM for all three PROTACs (Figure 2). However, at 10.0 μM , **BMM-3** and **BMM-4** induced the significant degradation of Bcl-X_L and **BMM-4** showed slightly higher activity. The results suggested that the linker is critical for degradation activity. Furthermore, **BMM-3** and

BMM-4 displayed degradation selectivity toward Bcl-X_L over BCL-2, but noticeable degradation for BCL-2 was also observed with **BMM-4**. The observations are consistent with VHL-based BCL-X_L PROTACs.^{12, 36}

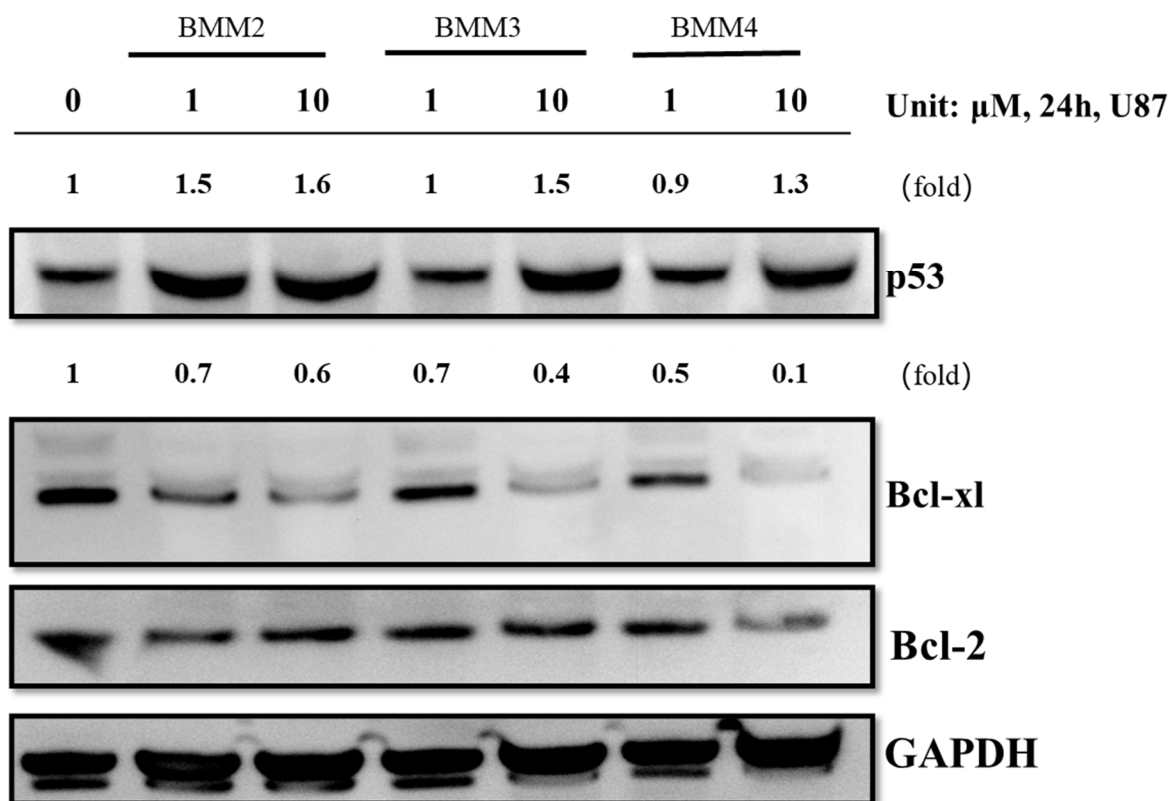


Figure 2. Degradation of Bcl-X_L by BMM PROTACs in U87 cells. Representative western blot analysis of Bcl-X_L, Bcl-2, and p53 protein levels in U87 after treatment with indicated concentrations of **BMM-2-4** PROTACs for 24 h.

The BMM PROTACs used Nutlin-3 as a ligand to recruit E3 ligase. Nutlin-3 is also a MDM2 inhibitor.³⁷ Inhibition of MDM2 protein blocks MDM2-p53 interaction, up-regulates the expression of p53 and thus exerts antitumor activity.²⁷⁻²⁹ Therefore we probed the p53 expression level. After 24 h, immunoblotting for p53 level in the U87 cells treated with **BMM-2**, **BMM-3** or **BMM-4** revealed a significant increase at 10.0 μ M (Figure 2). These results suggest that our designed compounds are also inhibitors of MDM2 because the Nutlin-3 is not touched and the solvent exposed site for linker connection has limited impact on its activity.

Further optimization of protocols revealed the degradation activity of the PROTACs was concentration and time dependent. **BMM-4** at 10.0 μM showed the best degraded ability and the stabilization of p53 (Figure 3a). We then studied the relationship of the degradation and the incubation time at 10 μM **BMM-4**. When the incubation time is more than 16 h gives more significant degradation (Figure 3c). Interestingly, the degradation activity did not lead to significant cell apoptosis (Figure 3d).

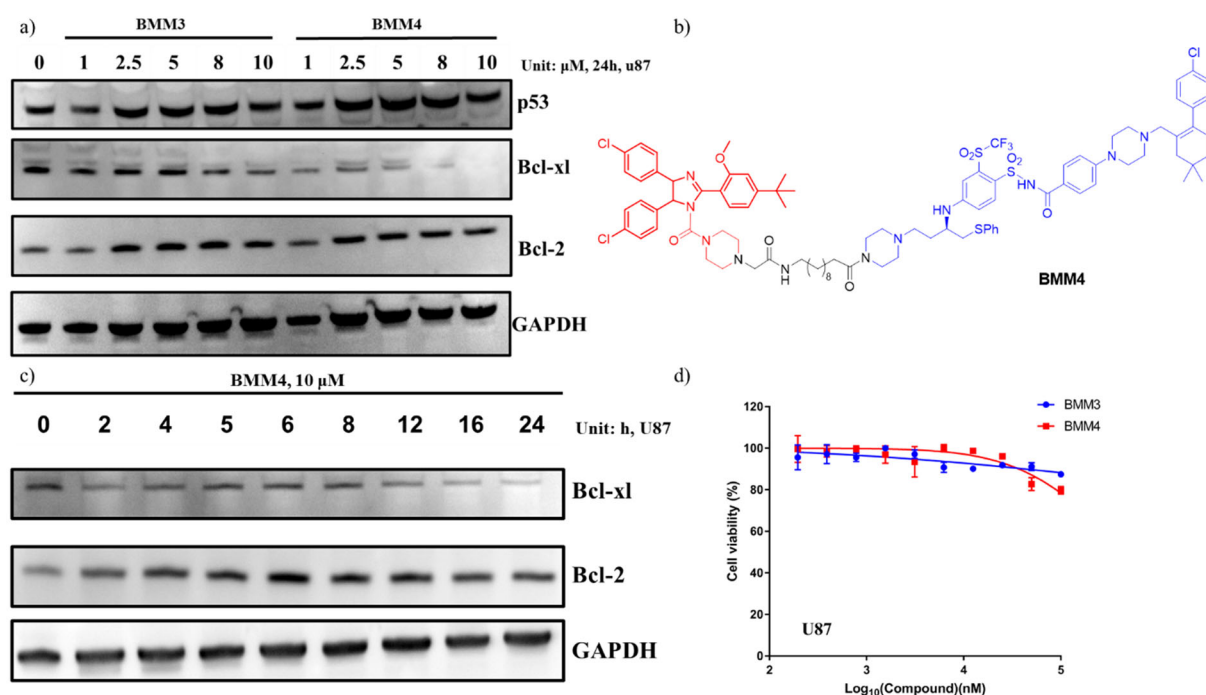


Figure 3. U87 cells were treated with different concentration or incubation time of **BMM-4**. a) Representative immunoblots from U87 cells treated with **BMM-4** at various concentrations. b) The structure of **BMM-4**. c) Representative immunoblots from U87 cells treated with 10.0 μM **BMM-4** for increasing incubation time. d) The cell viability of U87 cells treated with **BMM-3** and **BMM-4**.

Degradation activity in A549 cells

To demonstrate the sensitivity and generality of the **BMM** PROTACs, we explored the Bcl-XL degradation activity in A549 non-small cell lung cancer cell lines. The overexpression of Bcl-XL protein in A549 is the critical inhibitor of apoptosis, resulting in the poor prognosis.³⁸⁻³⁹ We also

found that **BMM4** effectively degraded Bcl-X_L in A549 cells with 10.0 μ M (Figure 4a). Furthermore, increase of p53 level was observed. However, different with the results obtained from U87, deletion of Bcl-X_L decreased the cell viability dramatically in the A549 cells (IC₅₀ = 4.99 μ M, Figure 4b.). Taken together, these results indicated that **BMM-4** degraded Bcl-X_L largely in different cancer cell lines.

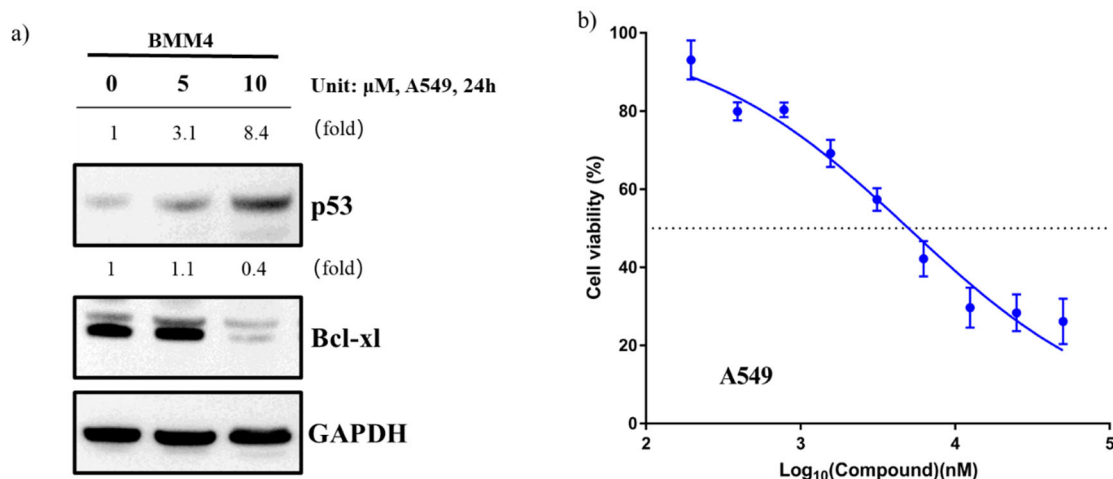


Figure 4. a) Degradation of Bcl-X_L by **BMM-4** in A549 cells. b) The cell viability of A549 cells treated with **BMM-4**.

Synergistic anticancer activity of **BMM-4** in combination with Bcl-2 inhibitor ABT-199

Previous studies have shown that most acute leukemias express wild-type p53, with defects in the p53 pathway preventing p53 from performing its tumor-suppressing tasks.⁴⁰ Meanwhile, MV-4-11, one of the commonly used acute myeloid leukemia cell lines, was sensitive to Bcl-2 inhibitor ABT-199.⁴¹ We questioned whether combining **BMM-4** with ABT-199 could have more effective cytotoxic activity than **BMM-4** alone in MV-4-11 cells. The western blot assay suggested **BMM-4** effectively degraded BCL-X_L and increased the p53 level at 10.0 μ M (Figure 5a). The cell viability assay revealed that significant synergistic effect was observed when co-administration of ABT-199 with **BMM-4**, resulting in significant cell apoptosis (Figure 5b). Given the Bcl-2 family proteins play an important role in inhibiting the tumor apoptosis, we performed flow cytometric analysis to evaluate the antitumor ability of **BMM-4** (Figure 5c and 5d). It was found that compound **BMM-4** induced 21.9% early apoptosis (Q3) in MV-4-11 cells at 10.0 μ M after 48 h treatment. The early apoptosis (Q3) of control group is just 6.25%. In addition, ABT-199 and

BMM-4 in combination increased the early apoptosis (Q3) to 34.5% under the same conditions. These results suggested that **BMM-4** induced MV-4-11 cells apoptosis and combining **BMM-4** with ABT-199 showed a more potent cytotoxic activity.

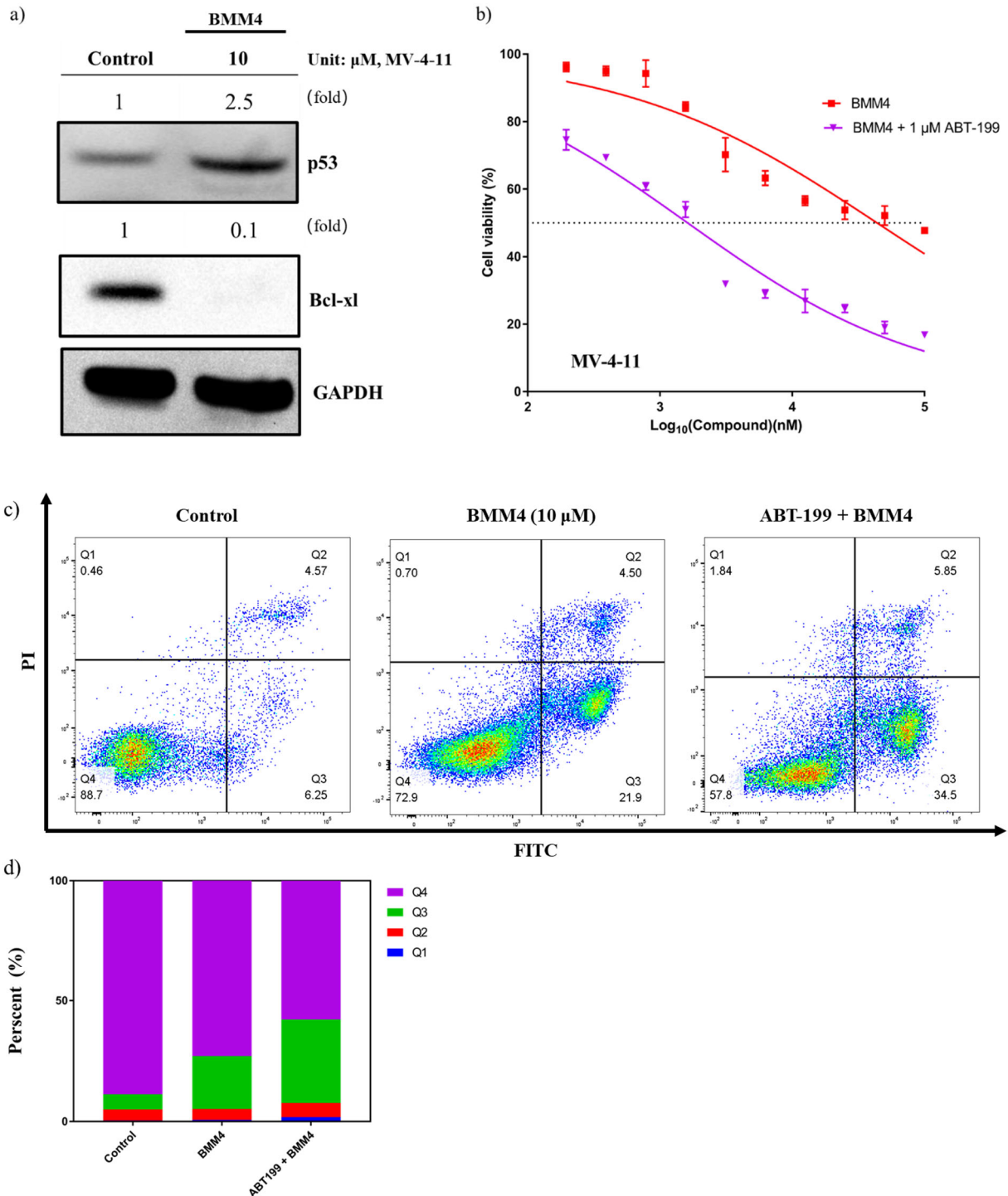


Figure 5. a) Degradation of Bcl-X_L by **BMM-4** in MV-4-11 cells. b) The cell viability of MV-4-11 treated with **BMM-4** or combined with 1.0 μM ABT-199. c, d) The characterization of apoptosis induced by compound **BMM-4** or **BMM-4** with ABT-199 in the MV-4-11 cell line.

Discussion and Conclusion

In consideration of the critical roles of Bcl family proteins and MDM2 in cancers, we developed a new class of PROTACs for targeting Bcl-X_L. MDM2 was explored as E3 ligase for degradation of Bcl-X_L for the first time. Three Nutlin-ABT-263 derived PROTACs were designed, synthesized and evaluated. Compound **BMM-4** was identified as the most promising degrader. Furthermore, different from the reported Bcl-targeting PROTACs, MDM2 PROTACs **BMM-4** exhibited unique dual activity. It selectively degraded Bcl-X_L and stabilized and enhanced p53 activity despite the fact that ABT-263 is a potent inhibitor for both Bcl-2 and Bcl-X_L. This suggests that **BMM-4** not only functionalized as an E3 ligase recruiter but also a MDM2 inhibitor. In addition, **BMM-4** showed high and broad sensitivity toward cancer cells, as shown in U87, A549 and MV-4-11 cancer cell lines. Furthermore, when compared to treatment with **BMM-4** alone, combination of **BMM-4** and BCL-2 inhibitor ABT-199 showed more potent antiproliferative activity. This may attribute to Bcl-2 and Bcl-X_L proteins, which are both regularly involved in the survival of tumors. It was also found that the linker plays important roles in degradation activity. A recent study from Zhou et al.¹⁶ by changing the linker position generated the dual degradation of Bcl-2 and Bcl-X_L instead of the single degradation of Bcl-X_L. Further studies need to be conducted to find dual degradation PROTACs for both Bcl-2 and Bcl-X_L via modification of the linker structures, which could influence the selectivity and activity toward Bcl-2 and Bcl-X_L. This represents the our future direction in this research.

Experimental Methods

General information

Commercially available reagents were purchased from Sigma Aldrich, Matrix Chemical, AKSci, Alfa Aesar, TCI, and Chem Cruz, and used as received unless otherwise noted. Merck 60 silica gel was used for chromatography, and Whatman silica gel plates with a fluorescence F254 indicator were used for thin-layer chromatography (TLC) analysis. ¹H and ¹³C NMR spectra were recorded on Bruker Advance 400. Chemical shifts in ¹H NMR spectra are reported in parts per million (ppm) relative to residual chloroform (7.26 ppm) or dimethyl sulfoxide (2.50 ppm) as internal standards. ¹H NMR data are reported as follows: chemical shift, multiplicity (s = singlet, d = doublet, m = multiplet), coupling constant in Hertz (Hz) and hydrogen numbers based on integration intensities. ¹³C NMR chemical shifts are reported in ppm relative to the central peak of CDCl₃ (77.16 ppm) as internal standards.

Key intermediate **12** was synthesized according to the procedures reported in literature.³⁴

tert-Butyl (R)-(7-(4-(3-((4-(N-(4-(4-((4'-chloro-4,4-dimethyl-3,4,5,6-tetrahydro-[1,1'-biphenyl]-2-yl)methyl)piperazin-1-yl)benzoyl)sulfamoyl)-2-((trifluoromethyl)sulfonyl)phenyl)amino)-4-(phenylthio)butyl)piperazin-1-yl)-7-oxoheptyl)carbamate (14). To a solution of 7-((tert-butoxycarbonyl)amino)heptanoic acid (**13**, 13.9 mg, 0.056 mmol) in DCM was added HATU (23.4 mg, 0.062 mmol), TEA (15.6 mg, 0.154 mmol), and compound **12** (50 mg, 0.051 mmol). The reaction was stirred at room temperature for 1 h and quenched by water. The organic layer was collected, washed by brine, dried over Na₂SO₄ and concentrated under vacuum. The residue was purified by reverse phase chromatography to afford the title compound (44 mg, 71%). LC–MS (ESI): m/z 1200.4 [M + H]⁺.

(R)-N-((4-((4-(4-(7-Aminoheptanoyl)piperazin-1-yl)-1-(phenylthio)butan-2-yl)amino)-3-((trifluoromethyl)sulfonyl)phenyl)sulfonyl)-4-(4-((4'-chloro-4,4-dimethyl-3,4,5,6-tetrahydro-[1,1'-biphenyl]-2-yl)methyl)piperazin-1-yl)benzamide (15). To a solution of compound **14** (44 mg, 0.037 mmol) in DCM was added TFA (1 mL) and the reaction was stirred at room temperature overnight. The resulting mixture was concentrated under vacuum and used directly for the next step without purification (quantitative). LC–MS (ESI): m/z 1100.4 [M + H]⁺.

N-((4-(((2R)-4-(4-(7-(2-(4-(2-(4-(tert-Butyl)-2-ethoxyphenyl)-4,5-bis(4-chlorophenyl)-4,5-dihydro-1H-imidazole-1-carbonyl)piperazin-1-yl)acetamido)heptanoyl)piperazin-1-yl)-1-(phenylthio)butan-2-yl)amino)-3-((trifluoromethyl)sulfonyl)phenyl)sulfonyl)-4-(4-((4'-chloro-4,4-dimethyl-3,4,5,6-

tetrahydro-[1,1'-biphenyl]-2-yl)methyl)piperazin-1-yl)benzamide (BMM-2). To a solution of compound **15** ($n = 5$, 10 mg, 0.016 mmol) in DMF was added HATU (7.2 mg, 0.019 mmol), TEA (4.8 mg, 0.047 mmol) and compound **16** (19.0 mg, 0.17 mmol). The resulting mixture was stirred at room temperature for 4 h and then quenched by water. The aqueous layer was extracted by ethyl acetate and the combined organic layers were dried over Na_2SO_4 and concentrated under vacuum. The residue was purified by reverse phase chromatography to afford the title compound (14 mg, 52%). ^1H NMR (500 MHz, Methanol- d_4) δ 8.29 (d, $J = 2.3$ Hz, 1H), 8.05 (dd, $J = 9.3, 2.3$ Hz, 1H), 7.79 – 7.74 (m, 2H), 7.72 – 7.68 (m, 1H), 7.41 – 7.36 (m, 2H), 7.36 – 7.30 (m, 4H), 7.28 – 7.23 (m, 2H), 7.22 – 7.17 (m, 4H), 7.17 – 7.11 (m, 5H), 7.05 (d, $J = 8.2$ Hz, 2H), 6.98 (d, $J = 9.1$ Hz, 2H), 6.93 (d, $J = 9.5$ Hz, 1H), 6.27 (d, $J = 11.2$ Hz, 1H), 6.04 (d, $J = 11.2$ Hz, 1H), 4.38 – 4.27 (m, 2H), 4.14 – 4.07 (m, 3H), 3.69 (s, 2H), 3.57 – 3.45 (m, 6H), 3.37 – 3.32 (m, 3H), 3.25 – 3.10 (m, 7H), 3.06 – 2.76 (m, 9H), 2.74 – 2.68 (m, 1H), 2.43 – 2.37 (m, 2H), 2.33 – 2.27 (m, 2H), 2.22 – 2.09 (m, 1H), 2.06 (s, 2H), 1.97 – 1.87 (m, 1H), 1.82 – 1.74 (m, 2H), 1.73 – 1.66 (m, 2H), 1.62 – 1.53 (m, 4H), 1.52 – 1.45 (m, 4H), 1.41 (s, 9H), 1.35 – 1.27 (m, 4H), 1.06 (s, 6H). LC-MS (ESI): m/z 1718.5 $[\text{M} + \text{H}]^+$.

***N*-(((4-(((2*R*)-4-(4-(9-(2-(4-(2-(4-(tert-Butyl)-2-ethoxyphenyl)-4,5-bis(4-chlorophenyl)-4,5-dihydro-1*H*-imidazole-1-carbonyl)piperazin-1-yl)acetamido)nonanoyl)piperazin-1-yl)-1-(phenylthio)butan-2-yl)amino)-3-((trifluoromethyl)sulfonyl)phenyl)sulfonyl)-4-(4-((4'-chloro-4,4-dimethyl-3,4,5,6-tetrahydro-[1,1'-biphenyl]-2-yl)methyl)piperazin-1-yl)benzamide (BMM-3).** The preparation of **BMM-2** was similar to compound **BMM-3**. ^1H NMR (500 MHz, Methanol- d_4) δ 8.29 (d, $J = 2.2$ Hz, 1H), 8.06 (dd, $J = 9.3, 2.3$ Hz, 1H), 7.77 (d, $J = 8.7$ Hz, 2H), 7.68 (d, $J = 8.1$ Hz, 1H), 7.42 – 7.37 (m, 2H), 7.36 – 7.30 (m, 4H), 7.25 (d, $J = 8.3$ Hz, 2H), 7.23 – 7.17 (m, 4H), 7.17 – 7.11 (m, 5H), 7.04 (d, $J = 8.2$ Hz, 2H), 6.98 (d, $J = 8.9$ Hz, 2H), 6.93 (d, $J = 9.5$ Hz, 1H), 6.26 (d, $J = 11.2$ Hz, 1H), 6.00 (d, $J = 11.2$ Hz, 1H), 4.36 – 4.29 (m, 2H), 4.14 – 4.07 (m, 3H), 3.69 (s, 2H), 3.51 – 3.37 (m, 6H), 3.29 – 3.13 (m, 8H), 3.12 – 3.06 (m, 2H), 2.88 – 2.50 (m, 10H), 2.43 – 2.37 (m, 2H), 2.30 (t, $J = 7.4$ Hz, 2H), 2.16 – 2.04 (m, 3H), 1.91 – 1.81 (m, 1H), 1.80 – 1.73 (m, 2H), 1.72 – 1.66 (m, 2H), 1.62 – 1.53 (m, 4H), 1.50 (t, $J = 7.0$ Hz, 4H), 1.47 – 1.44 (m, 1H), 1.41 (s, 9H), 1.34 – 1.25 (m, 8H), 1.06 (s, 6H). LC-MS (ESI): m/z 1746.6 $[\text{M} + \text{H}]^+$.

***N*-(((4-(((2*R*)-4-(4-(11-(2-(4-(2-(4-(tert-Butyl)-2-ethoxyphenyl)-4,5-bis(4-chlorophenyl)-4,5-dihydro-1*H*-imidazole-1-carbonyl)piperazin-1-yl)acetamido)undecanoyl)piperazin-1-yl)-1-(phenylthio)butan-2-yl)amino)-3-((trifluoromethyl)sulfonyl)phenyl)sulfonyl)-4-(4-((4'-chloro-4,4-dimethyl-3,4,5,6-tetrahydro-[1,1'-biphenyl]-2-yl)methyl)piperazin-1-yl)benzamide (BMM-4).** The preparation of **BMM-4** was similar to compound **BMM-2**. ^1H NMR (500 MHz, Methanol- d_4) δ 8.28 (d, $J = 2.2$ Hz, 1H), 8.06 (dd, $J = 9.3, 2.3$ Hz, 1H), 7.77 (d, $J = 8.6$ Hz, 2H), 7.67 (d, $J = 8.1$ Hz, 1H), 7.42 – 7.37 (m, 2H), 7.35 – 7.29 (m, 4H), 7.28 – 7.23 (m, 2H), 7.23 – 7.17 (m, 4H), 7.17 – 7.11 (m, 5H), 7.03 (d, $J =$

8.1 Hz, 2H), 6.98 (d, J = 8.9 Hz, 2H), 6.93 (d, J = 9.5 Hz, 1H), 6.25 (d, J = 11.3 Hz, 1H), 5.99 (d, J = 11.2 Hz, 1H), 4.35 – 4.28 (m, 2H), 4.14 – 4.07 (m, 3H), 3.69 (s, 2H), 3.49 – 3.36 (m, 6H), 3.25 – 3.14 (m, 8H), 3.11 – 3.07 (m, 2H), 2.80 – 2.43 (m, 10H), 2.42 – 2.38 (m, 2H), 2.30 (t, J = 7.5 Hz, 2H), 2.14 – 2.04 (m, 3H), 1.90 – 1.82 (m, 1H), 1.80 – 1.74 (m, 2H), 1.73 – 1.67 (m, 2H), 1.62 – 1.55 (m, 4H), 1.50 (t, J = 7.0 Hz, 3H), 1.47 – 1.44 (m, 1H), 1.41 (s, 9H), 1.31 – 1.24 (m, 12H), 1.06 (s, 6H). LC-MS (ESI): m/z 1774.5 [M + H]⁺.

Cell Culture

U87-MG cells and A549 were maintained in Dulbecco's modified Eagle's medium (DMEM, Cat. No. 10-013-cv) containing 10% FBS, 100 units/mL of penicillin, and 100 µg/mL streptomycin (Cat. No. 30-002-CI). The cells were grown at 37 °C with 5% CO₂. MV-4-11 was maintained in RPMI 1640 containing 10% FBS.

Cell Viability Assay

Tumor cells were plated in 96-well plates with 6.0×10^3 cells in each well and subsequently incubated for 24 h in a moist atmosphere of 5% CO₂ and 37 °C. Then, different concentrations of test compounds or vehicles were added to triplicate wells. After incubation for an additional 72 h, 10 µL CCK-8 solution (Dojindo Molecular Technologies, Cat. No. CK04-11) was added to each well, then the plates were incubated for 4 h at 37 °C. The absorbance was read at 450 nm on a Microplate Reader (Molecular Devices). The values of IC₅₀ were calculated by the Logit method with the GraphPad software.

Antibodies

Anti-Bcl-xl antibody was purchased from Thermo Fisher Scientific (Cat. No. 66020-1-IG). Anti-Bcl-2 antibody was purchased from Thermo Fisher Scientific (Cat. No. MA5-11757). Anti-GAPDH antibody was purchased from Sigma-Aldrich (Cat. No. G8795). Anti-p53 antibody was purchased from Sigma-Aldrich (Cat. No. P6874). All primary antibodies were used at a suggested dilution in 5% non-fat milk in Phosphate-buffered saline with 0.1% Tween-20 (PBST) buffer for western blot assay. All secondary antibodies were used at a 1:4000 dilution in 5% non-fat milk in Phosphate-buffered saline with 0.1% Tween-20 (PBST) buffer for western blot assay.

Immunoblot Assay

Cells were lysed in RIPA buffer supplemented with protease inhibitors. The lysates (40-60 μ g protein) were then resolved by 4%-12% Mini Protein Gel (Thermo Fisher, Cat. No. NP0322BOX) at 70 V for 10 mins and 150 V for 40 mins. Then the proteins were transferred from the gel to PVDF membrane (Bio-Rad, Cat. No. 1620177) at 20 V for 120 mins. The membrane was incubated with primary antibody at 4 °C overnight, washed 3 times with PBST, incubated secondary antibody in 5% nonfat milk for 60 mins at room temperature and then washed 3 times with PBST.

Apoptosis Assay

MV-4-11 cells (5×10^4 cells/well) were placed in 6-well transparent plates and then treated with test compounds and vehicle in a moist atmosphere of 5% CO₂ at 37 C for 48 h. After that, Annexin V-fluorescein isothiocyanate (FITC, 5 μ L, BioLegend) was added to the resuspended cell solution, which was then incubated for 15 min at room temperature. After adding 10 μ L PI (BioLegend), the treated cells were incubated for another 15 min in the dark at room temperature. The analysis of stained cells was performed by a flow cytometer.

Acknowledgements

The research is supported by NIH 5R01GM130772, the Pharmaceutical Research and Manufacturers of America Foundation (PhRMA Foundation), R. Ken Coit College of Pharmacy and Arizona Center for Drug Discovery at the University of Arizona.

Conflict of interest

The authors declare that they have no known competing financial interests or personal relationships that could have appeared to influence the work reported in this paper.

References

1. Hanahan, D.; Weinberg, R. A., Hallmarks of cancer: the next generation. *Cell* **2011**, *144* (5), 646-74.
2. Singh, R.; Letai, A.; Sarosiek, K., Regulation of apoptosis in health and disease: the balancing act of BCL-2 family proteins. *Nat Rev Mol Cell Biol* **2019**, *20* (3), 175-193.
3. Delbridge, A. R.; Grabow, S.; Strasser, A.; Vaux, D. L., Thirty years of BCL-2: translating cell death discoveries into novel cancer therapies. *Nat Rev Cancer* **2016**, *16* (2), 99-109.
4. Elmore, S., Apoptosis: A Review of Programmed Cell Death. *Toxicol. Pathol.* **2007**, *35*, 495–516.
5. Tang, D.; Kang, R.; Berghe, T. V.; Vandenabeele, P.; Kroemer, G., The molecular machinery of regulated cell death. *Cell Res.* **2019**, *29*, 347–364.
6. Singh, R.; Letai, A.; Sarosiek, K., Regulation of apoptosis in health and disease: the balancing act of BCL-2 family proteins. *Nat. Rev. Mol. Cell Biol.* **2019**, *20*, 175-193.
7. Igney, F. H.; Krammer, P. H., Death and anti-death: tumour resistance to apoptosis. *Nat. Rev. Cancer* **2002**, *2*, 277–288.
8. Rudin, C. M.; Hann, C. L.; Garon, E. B.; Ribeiro de Oliveira, M.; Bonomi, P. D.; Camidge, D. R.; Chu, Q.; Giaccone, G.; Khaira, D.; Ramalingam, S. S.; Ranson, M. R.; Dive, C.; McKeegan, E. M.; Chyla, B. J.; Dowell, B. L.; Chakravarty, A.; Nolan, C. E.; Rudersdorf, N.; Busman, T. A.; Mabry, M. H.; Krivoshik, A. P.; Humerickhouse, R. A.; Shapiro, G. I.; Gandhi, L., Phase II study of single-agent navitoclax (ABT-263) and biomarker correlates in patients with relapsed small cell lung cancer. *Clin Cancer Res* **2012**, *18* (11), 3163-9.
9. Garner, T. P.; Lopez, A.; Reyna, D. E.; Spitz, A. Z.; Gavathiotis, E., Progress in targeting the BCL-2 family of proteins. *Curr Opin Chem Biol* **2017**, *39*, 133-142.
10. Kaefer, A.; Yang, J.; Noertersheuser, P.; Mensing, S.; Humerickhouse, R.; Awni, W.; Xiong, H., Mechanism-based pharmacokinetic/pharmacodynamic meta-analysis of navitoclax (ABT-263) induced thrombocytopenia. *Cancer Chemother Pharmacol* **2014**, *74* (3), 593-602.
11. Zhang, X.; Thummuri, D.; Liu, X.; Hu, W.; Zhang, P.; Khan, S.; Yuan, Y.; Zhou, D.; Zheng, G., Discovery of PROTAC BCL-XL degraders as potent anticancer agents with low on-target platelet toxicity. *Eur J Med Chem* **2020**, *192*, 112186.

12. Pal, P.; Thummuri, D.; Lv, D.; Liu, X.; Zhang, P.; Hu, W.; Poddar, S. K.; Hua, N.; Khan, S.; Yuan, Y.; Zhang, X.; Zhou, D.; Zheng, G., Discovery of a Novel BCL-XL PROTAC Degradator with Enhanced BCL-2 Inhibition. *J Med Chem* **2021**, *64* (19), 14230-14246.
13. Bekes, M.; Langley, D. R.; Crews, C. M., PROTAC targeted protein degraders: the past is prologue. *Nat Rev Drug Discov* **2022**, *21* (3), 181-200.
14. Bondeson, D. P.; Mares, A.; Smith, I. E.; Ko, E.; Campos, S.; Miah, A. H.; Mulholland, K. E.; Routly, N.; Buckley, D. L.; Gustafson, J. L.; Zinn, N.; Grandi, P.; Shimamura, S.; Bergamini, G.; Faeltz-Savitski, M.; Bantscheff, M.; Cox, C.; Gordon, D. A.; Willard, R. R.; Flanagan, J. J.; Casillas, L. N.; Votta, B. J.; den Besten, W.; Famm, K.; Kruidenier, L.; Carter, P. S.; Harling, J. D.; Churcher, I.; Crews, C. M., Catalytic in vivo protein knockdown by small-molecule PROTACs. *Nat Chem Biol* **2015**, *11* (8), 611-7.
15. Bondeson, D. P.; Smith, B. E.; Burslem, G. M.; Buhimschi, A. D.; Hines, J.; Jaime-Figueroa, S.; Wang, J.; Hamman, B. D.; Ishchenko, A.; Crews, C. M., Lessons in PROTAC Design from Selective Degradation with a Promiscuous Warhead. *Cell Chem Biol* **2018**, *25* (1), 78-87 e5.
16. Lv, D.; Pal, P.; Liu, X.; Jia, Y.; Thummuri, D.; Zhang, P.; Hu, W.; Pei, J.; Zhang, Q.; Zhou, S.; Khan, S.; Zhang, X.; Hua, N.; Yang, Q.; Arango, S.; Zhang, W.; Nayak, D.; Olsen, S. K.; Weintraub, S. T.; Hromas, R.; Konopleva, M.; Yuan, Y.; Zheng, G.; Zhou, D., Development of a BCL-xL and BCL-2 dual degrader with improved anti-leukemic activity. *Nat Commun* **2021**, *12* (1), 6896.
17. Mattioli, F.; Sixma, T. K., Lysine-targeting specificity in ubiquitin and ubiquitin-like modification pathways. *Nat Struct Mol Biol* **2014**, *21* (4), 308-16.
18. Hines, J.; Lartigue, S.; Dong, H.; Qian, Y.; Crews, C. M., MDM2-Recruiting PROTAC Offers Superior, Synergistic Antiproliferative Activity via Simultaneous Degradation of BRD4 and Stabilization of p53. *Cancer Res* **2019**, *79* (1), 251-262.
19. Honda, R.; Tanaka, H.; Yasuda, H., Oncoprotein MDM2 is a ubiquitin ligase E3 for tumor suppressor p53. *FEBS Lett* **1997**, *420* (1), 25-7.
20. Han, X.; Wei, W.; Sun, Y., PROTAC degraders with ligands recruiting MDM2 E3 ubiquitin ligase: an updated perspective. *Acta Materia Medica* **2022**, *1*, 244-259.
21. Moll, U. M.; Petrenko, O., The MDM2-p53 interaction. *Mol Cancer Res* **2003**, *1* (14), 1001-8.

22. Harris, C. C., p53 tumor suppressor gene: from the basic research laboratory to the clinic--an abridged historical perspective. *Carcinogenesis* **1996**, *17* (6), 1187-98.
23. el-Deiry, W. S., Regulation of p53 downstream genes. *Semin Cancer Biol* **1998**, *8* (5), 345-57.
24. Momand, J.; Wu, H. H.; Dasgupta, G., MDM2--master regulator of the p53 tumor suppressor protein. *Gene* **2000**, *242* (1-2), 15-29.
25. Perry, M. E., The regulation of the p53-mediated stress response by MDM2 and MDM4. *Cold Spring Harb Perspect Biol* **2010**, *2* (1), a000968-a000968.
26. Vassilev, L. T.; Vu, B. T.; Graves, B.; Carvajal, D.; Podlaski, F.; Filipovic, Z.; Kong, N.; Kammlott, U.; Lukacs, C.; Klein, C.; Fotouhi, N.; Liu, E. A., In vivo activation of the p53 pathway by small-molecule antagonists of MDM2. *Science* **2004**, *303* (5659), 844-848.
27. Hines, J.; Lartigue, S.; Dong, H.; Qian, Y.; Crews, C. M., MDM2-Recruiting PROTAC Offers Superior, Synergistic Antiproliferative Activity via Simultaneous Degradation of BRD4 and Stabilization of p53. *Cancer Res* **2019**, *79* (1), 251-262.
28. Wurz, R. P.; Cee, V. J., Targeted Degradation of MDM2 as a New Approach to Improve the Efficacy of MDM2-p53 Inhibitors. *J Med Chem* **2019**, *62* (2), 445-447.
29. Wang, B.; Wu, S.; Liu, J.; Yang, K.; Xie, H.; Tang, W., Development of selective small molecule MDM2 degraders based on nutlin. *Eur J Med Chem* **2019**, *176*, 476-491.
30. Wang, S.; Zhao, Y.; Aguilar, A.; Bernard, D.; Yang, C.-Y., Targeting the MDM2-p53 Protein-Protein Interaction for New Cancer Therapy: Progress and Challenges. *Cold Spring Harb Perspect Med* **2017**, *7* (5), a026245.
31. Zhao, Y.; Aguilar, A.; Bernard, D.; Wang, S., Small-molecule inhibitors of the MDM2-p53 protein-protein interaction (MDM2 Inhibitors) in clinical trials for cancer treatment. *J Med Chem* **2015**, *58* (3), 1038-1052.
32. Vassilev, L. T.; Vu, B. T.; Graves, B.; Carvajal, D.; Podlaski, F.; Filipovic, Z.; Kong, N.; Kammlott, U.; Lukacs, C.; Klein, C.; Fotouhi, N.; Liu, E. A., In vivo activation of the p53 pathway by small-molecule antagonists of MDM2. *Science* **2004**, *303*, 844-848.
33. He, S.-P.; Ma, J.; Fang, Y.; Liu, Y.; Wu, S.; Dong, G.; Wang, W.; Sheng, C., Homo-PROTAC Mediated Suicide of MDM2 to Treat Non-small Cell Lung Cancer. *Acta Pharm. Sin. B* **2021**, *10*, 1617-1628.

34. Wang, G.; Zhang, H.; Zhou, J.; Ha, C.; Pei, D.; Ding, K., An Efficient Synthesis of ABT-263, a Novel Inhibitor of Antiapoptotic Bcl-2 Protein. *Synthesis* **2008**, 2398–2404.
35. Wu, S.; Zhou, Y.; Yang, G.; Tian, H.; Geng, Y.; Hu, Y.; Lin, K.; Wu, W., Sulforaphane-cysteine induces apoptosis by sustained activation of ERK1/2 and caspase 3 in human glioblastoma U373MG and U87MG cells. *Oncol Rep* **2017**, *37* (5), 2829-2838.
36. Khan, S.; Zhang, X.; Lv, D.; Zhang, Q.; He, Y.; Zhang, P.; Liu, X.; Thummuri, D.; Yuan, Y.; Wiegand, J. S.; Pei, J.; Zhang, W.; Sharma, A.; McCurdy, C. R.; Kuruvilla, V. M.; Baran, N.; Ferrando, A. A.; Kim, Y. M.; Rogojina, A.; Houghton, P. J.; Huang, G.; Hromas, R.; Konopleva, M.; Zheng, G.; Zhou, D., A selective BCL-XL PROTAC degrader achieves safe and potent antitumor activity. *Nat Med* **2019**, *25* (12), 1938-1947.
37. Vassilev, L. T.; Vu, B. T.; Graves, B.; Carvajal, D.; Podlaski, F.; Filipovic, Z.; Kong, N.; Kammlott, U.; Lukacs, C.; Klein, C.; Fotouhi, N.; Liu, E. A., In vivo activation of the p53 pathway by small-molecule antagonists of MDM2. *Science* **2004**, *303* (5659), 844-8.
38. Othman, N.; In, L. L.; Harikrishna, J. A.; Hasima, N., Bcl-xL silencing induces alterations in hsa-miR-608 expression and subsequent cell death in A549 and SK-LU1 human lung adenocarcinoma cells. *PLoS One* **2013**, *8* (12), e81735.
39. Yang, C.; Huang, W.; Yan, L.; Wang, Y.; Wang, W.; Liu, D.; Zuo, X., Downregulation of the expression of Bcell lymphoma-extra large by RNA interference induces apoptosis and enhances the radiosensitivity of nonsmall cell lung cancer cells. *Mol Med Rep* **2015**, *12* (1), 449-55.
40. Kojima, K.; Ishizawa, J.; Andreeff, M., Pharmacological activation of wild-type p53 in the therapy of leukemia. *Exp Hematol* **2016**, *44* (9), 791-798.
41. Levenson, J. D.; Phillips, D. C.; Mitten, M. J.; Boghaert, E. R.; Diaz, D.; Tahir, S. K.; Belmont, L. D.; Nimmer, P.; Xiao, Y.; Ma, X. M.; Lowes, K. N.; Kovar, P.; Chen, J.; Jin, S.; Smith, M.; Xue, J.; Zhang, H.; Oleksijew, A.; Magoc, T. J.; Vaidya, K. S.; Albert, D. H.; Tarrant, J. M.; La, N.; Wang, L.; Tao, Z. F.; Wendt, M. D.; Sampath, D.; Rosenberg, S. H.; Tse, C.; Huang, D. C.; Fairbrother, W. J.; Elmore, S. W.; Souers, A. J., Exploiting selective BCL-2 family inhibitors to dissect cell survival dependencies and define improved strategies for cancer therapy. *Sci Transl Med* **2015**, *7* (279), 279ra40.